



RNA Sequencing of Human Peripheral Nerve in Response to Injury: Distinctive Analysis of the Nerve Repair Pathways

Cell Transplantation
 Volume 29: 1–13
 © The Author(s) 2020
 Article reuse guidelines:
sagepub.com/journals-permissions
 DOI: 10.1177/0963689720926157
journals.sagepub.com/home/ccl


Andrew S. Welleford^{1,2,*}, Jorge E. Quintero^{1,2,3,*}, Nader El Seblani^{1,2,4,*} , Eric Blalock^{1,2}, Sumedha Gunewardena⁵, Steven M. Shapiro^{6,7}, Sean M. Riordan⁶, Peter Huettl^{1,2}, Zain Guduru⁸, John A. Stanford⁷, Craig G. van Horne^{1,2,3}, and Greg A. Gerhardt^{1,2,3,8}

Abstract

The development of regenerative therapies for central nervous system diseases can likely benefit from an understanding of the peripheral nervous system repair process, particularly in identifying potential gene pathways involved in human nerve repair. This study employed RNA sequencing (RNA-seq) technology to analyze the whole transcriptome profile of the human peripheral nerve in response to an injury. The distal sural nerve was exposed, completely transected, and a 1 to 2 cm section of nerve fascicles was collected for RNA-seq from six participants with Parkinson's disease, ranging in age between 53 and 70 yr. Two weeks after the initial injury, another section of the nerve fascicles of the distal and pre-degenerated stump of the nerve was dissected and processed for RNA-seq studies. An initial analysis between the pre-lesion status and the postinjury gene expression revealed 3,641 genes that were significantly differentially expressed. In addition, the results support a clear transdifferentiation process that occurred by the end of the 2-wk postinjury. Gene ontology (GO) and hierarchical clustering were used to identify the major signaling pathways affected by the injury. In contrast to previous nonclinical studies, important changes were observed in molecular pathways related to antiapoptotic signaling, neurotrophic factor processes, cell motility, and immune cell chemotactic signaling. The results of our current study provide new insights regarding the essential interactions of different molecular pathways that drive neuronal repair and axonal regeneration in humans.

Keywords

RNA-seq; peripheral nerve; Schwann cell; graft; neurodegenerative diseases; Wallerian degeneration

¹ Department of Neuroscience, University of Kentucky Medical Center, Lexington, KY, USA

² Brain Restoration Center, University of Kentucky, Lexington, KY, USA

³ Department of Neurosurgery, University of Kentucky Medical Center, Lexington, KY, USA

⁴ Department of Pharmaceutical Sciences, University of Kentucky, Lexington, KY, USA

⁵ Kansas Intellectual and Developmental Disabilities Research Center, University of Kansas Medical Center, KS, USA

⁶ Division of Neurology, Department of Pediatrics, Children's Mercy Hospital, Kansas City, MO, USA

⁷ Department of Molecular and Integrative Physiology, University of Kansas Medical Center, KS, USA

⁸ Department of Neurology, University of Kentucky Medical Center, Lexington, KY, USA

* These are co-first authors and have contributed equally to this article

Submitted: December 9, 2019. Revised: April 18, 2020. Accepted: April 22, 2020.

Corresponding Author:

Greg A. Gerhardt, Department of Neuroscience, University of Kentucky Medical Center, 800 Rose Street, Room MN206 Medical Sciences Building, Lexington, KY 40536-0098, USA.

Email: gregg@uky.edu



Creative Commons Non Commercial CC BY-NC: This article is distributed under the terms of the Creative Commons Attribution-NonCommercial 4.0 License (<https://creativecommons.org/licenses/by-nc/4.0/>) which permits non-commercial use, reproduction and distribution of the work without further permission provided the original work is attributed as specified on the SAGE and Open Access pages (<https://us.sagepub.com/en-us/nam/open-access-at-sage>).

Introduction

In contrast to the central nervous system (CNS), the axons of the peripheral nervous system (PNS) are capable of regenerating after injury¹ and re-establishing functional connections with their distal target². This regeneration is enabled by the interaction between the injured axons, the nerve extracellular matrix, immune cells such as macrophages, and Schwann cells^{3,4}. These nerve components individually contribute to peripheral nerve repair and interact with each other to further support a functional regeneration⁵. Following an injury to a peripheral nerve, the distal stump undergoes a process known as Wallerian degeneration. Schwann cells, macrophages, and neutrophils are the key players in this process. Together they breakdown myelin debris and clear the severed axonal membrane and cytoskeleton⁶. Reprogrammed Schwann cells also communicate with the fibroblasts to synthesize major adhesion proteins and a new extracellular matrix, which helps in bridging the proximal and distal stumps of the injured nerve fibers (for review, see Jessen and Mirsky⁸). Under favorable conditions, the proximal segment of the injured axon sprouts new processes that reassociate with a new phenotype of Schwann cells, optimized for repair, and regenerate through the extracellular matrix of the distal nerve. In this way, the regenerating peripheral nerve fibers re-establish communication with the original distal target and restore some degree of function.

Myelinating and nonmyelinating (Remak) subtypes of Schwann cells undergo cellular reprogramming into a “repair” profile in response to PNS injury⁷. Repair Schwann cells shed their myelin, become mobile, and secrete trophic factors and other signaling molecules to promote axonal regeneration⁸. In response to an injury, Schwann cells release soluble growth factors such as nerve growth factor, brain-derived neurotrophic factor, insulin-like growth factor-1, hepatocyte growth factor, vascular endothelial growth factor, neurotrophin-3, and glial cell line-derived neurotrophic factor (GDNF)^{9–12}. These growth factors play a crucial role in inducing and guiding the regenerating distal end of the injured peripheral nerve fibers¹³.

Regulation of gene expression may be a therapeutic target for promoting the successful recovery of peripheral nerve after injury. Identification of those genes and how they interact is crucial to exploring strategies that enhance the neural protection, regeneration, and repair processes. Promoting successful regeneration in the CNS has been difficult in neurodegenerative diseases, traumatic brain injury, stroke, epilepsy, and other neurological disorders. We believe that understanding the gene expression changes that drive effective neural repair within the PNS may also help in identifying new therapeutic targets or methods that could enhance CNS neural regeneration.

Whole transcriptome profiling of gene expression in response to peripheral nerve injury can now be feasibly studied using RNA sequencing (RNA-seq) technology. RNA-seq combines molecular biology approaches for RNA

amplification with bioinformatics tools for measuring and validating large RNA-seq datasets. This technique allows for quantitative measurements of thousands of gene transcripts using small (10 to 30 mg or less) quantities of tissue. For a review of the applications of RNA-seq see Han et al¹⁴.

Our study was conducted in conjunction with an ongoing clinical trial (clinicaltrials.gov: NCT#02369003), the “DBS Plus” trial, which involves grafting of autologous peripheral nerve fascicles in patients with Parkinson’s disease (PD) at the time of deep brain stimulation (DBS) surgery¹⁵, an approach we call DPS Plus. To our knowledge, our study is the first of its type studying and analyzing the human peripheral nerve repair genetics in response to a transection injury within the same human subjects. The central hypothesis of this ongoing clinical trial is that the progression of motor symptoms of PD may be slowed and modified by providing a source of neuroprotective and pro-regenerative factors, i.e., autologous peripheral nerve tissue, to the degenerating dopaminergic neurons responsible for the motor deficits of PD. The trial involved collection of two samples of the sural nerve from the same participant at two distinct time points. The first sample, referred to as the “pre-lesion” sample, was collected from the participant’s sural nerve during Stage I of the surgery, which involved DBS hardware implantation. The second sample, referred to as the “post-lesion” sample, was taken 2 weeks later from the distal end of the same nerve during Stage II of the surgery, which is the stage when the DBS leads are positioned into the subthalamic nucleus (STN) or globus pallidus internus (GPi). This two-stage approach corresponds with the two stages of DBS surgery and was designed with the objective of inducing pro-regenerative changes in the peripheral nerve following an injury^{13,16}. This current study was performed to analyze the transcriptome profile of normal and transected sural nerve tissue in patients with PD and to help evaluate how a conditioning injury of peripheral nerve tissue can induce pro-regenerative changes.

Materials and Methods

Research Subjects

The nerve samples were collected from human subjects with PD who electively consented to participate in the clinical trial testing the safety and feasibility of peripheral nerve grafts to the brain for the treatment of PD. The consent allowed for the collection of sural nerve sample for research studies. The nerve samples of six participants (two females and four males), with a mean age of 64 ± 7 yr (mean \pm standard deviation [SD]) (range 53 to 70 yr) and with a diagnosed disease duration of 10 ± 5 yr (range 2 to 16 yr), were used for RNA-seq analysis.

Tissue Collection

The sural nerve samples were collected at two different time points: a pre-lesion sample was collected at the time of the

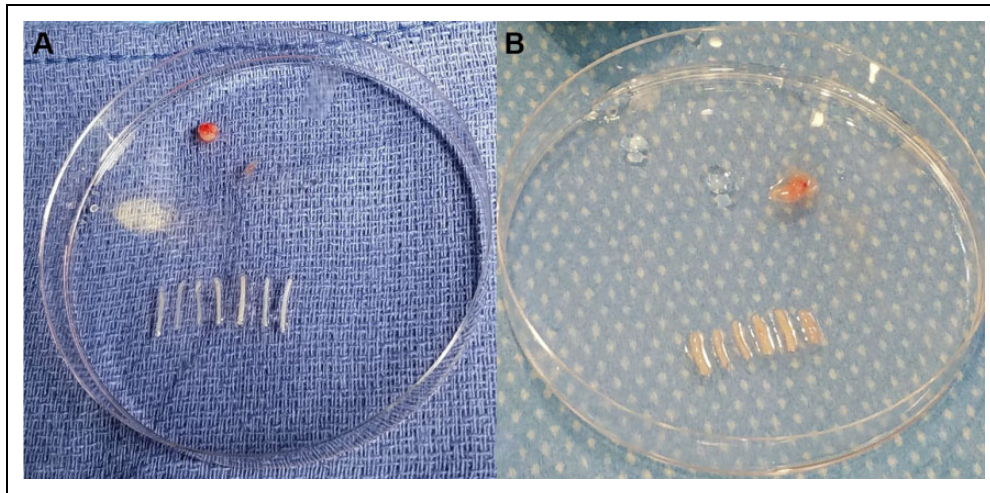


Fig. 1. Photographs of the peripheral nerve fascicles analyzed in this study. (A) The samples collected in Stage I of the DBS surgery (pre-lesion sample). (B) The samples collected in Stage II of the DBS surgery (post-lesion sample). DBS: deep brain stimulation.

first stage of DBS surgery (Stage I) followed by a post-lesion sample from the second stage of DBS surgery (Stage II) 2 weeks later^{17,18} (Fig. 1). Both nerve samples were collected before activating the DBS electrodes following the second stage of DBS surgery. For the pre-lesion tissue collection, the surgeon made a transverse incision through the skin of the lateral ankle, 2 cm superior to the lateral malleolus. The surgeon then identified the neurovascular bundle containing the sural nerve with the associated artery and vein. The sural nerve was then separated from the bundle using blunt dissection. Next, two black silk sutures were tied around the nerve, roughly 1 cm apart, to mark the nerve. The section of the sural nerve between these sutures was then cut, a 1-cm nerve segment was removed, and the surgical area was sutured and closed.

The removed section of nerve was then stripped of its epineurium using microsurgical dissection in cold sterile saline. Individual fascicles of nerve fibers were separated using jeweler's forceps, and the perineurium was discarded (Fig. 1). These fascicles were placed in conical microcentrifuge tubes, snap-frozen on dry ice, and stored at -80°C until they were assayed. For post-lesion tissue collection, the surgical area from Stage I was reopened at the original incision. The surgeon located the suture markers on the distal stump of the transected sural nerve and removed a new 1 to 2 cm segment of the remaining distal stump of the previously severed nerve. The tissue was kept on sterile saline ice and was prepared for the trial intervention as previously described¹⁷. Once the trial intervention was completed, the remaining fascicles (Fig. 1B) were placed in conical microcentrifuge tubes, snap-frozen on dry ice, and stored at -80°C until assayed.

RNA Extraction

RNA isolation was performed by homogenizing sural nerve fascicles in 1 ml of TRI Reagent Solution (ThermoFisher

AM9738, USA) using a Fisher Scientific Power Gen 35 homogenizer (Fisher Scientific PG35-362, USA) with a microtip homogenizing probe. The homogenized lysate was transferred to a pre-pelleted 5Prime Phase Lock Gel—Heavy 2 ml tube (ThermoFisher NC1093153, USA) and incubated at room temperature for 5 min. Two hundred microliters of chloroform (Sigma-Aldrich C2432, USA) was added and the tube was shaken vigorously by hand for 15 s. Phase separation was performed by microcentrifugation at $12,000 \times g$ for 10 min. The RNA containing aqueous phase was taken from the top of the Phase Lock Gel layer and transferred to a 1.7-ml microfuge tube. RNA was precipitated by adding 0.5 ml isopropyl alcohol {2-Propanol} (Sigma-Aldrich I9516, USA), mixed by repeated inversion, and incubated at room temperature for 10 min. RNA was pelleted by microcentrifugation at $12,000 \times g$ for 10 min at 4°C . RNA pellet was washed two times with 80% ethanol (Sigma-Aldrich E7023, USA) using a $7,500 \times g$ microcentrifugation for 5 min at 4°C to pellet RNA between washes. RNA pellets were air dried 5 to 10 min at room temperature and resuspended in 25 μl of nuclease-free water. RNA purity was assessed by OD260/OD280 ratio calculation using a ThermoFisher NanoDrop 1000 Spectrophotometer (ThermoFisher ND-1000, USA). RNA Integrity was assessed by Agilent Bioanalyzer 2100 (Agilent G2939BA, USA) using the Eukaryotic Total RNA Nano assay.

RNA Sequencing

RNA-Seq was performed at a strand-specific 100 cycle paired-end resolution, in an illumina HiSeq 2500 sequencing machine (Illumina, San Diego, CA, USA). In a repeated measure design, mRNA from the six individual samples were sequenced pre- and post-lesioning, thus, resulting in a total of 12 samples. The 12 samples were multiplexed in two lanes of a flow cell, resulting between 25 and 34 million

Table 1. Mass and Freezing Time Delay of the Nerve Samples Collected During Stage I vs Stage II.

Participant	Stage I samples		Stage II samples	
	Mass (g)	Freezing time delay (min)	Mass (g)	Freezing time delay (min)
1	0.0205	16	0.0354	41
2	0.0158	28	0.0301	108
3	0.0254	20	0.0613	64
4	0.0256	14	0.0363	52
5	0.0294	14	0.0757	39
6	0.0197	17	0.0256	50
Mean \pm SD	0.0227 \pm 0.0049	18 \pm 5	0.0441 \pm 0.0198	59 \pm 25

Freezing time delay includes the gross dissection time during which fascicles were separated from the whole nerve and the time required for fascicle segment grafting into participants during Stage II. SD: standard deviation.

reads per sample. The read quality was assessed using the FastQC software¹⁹. On average, the per sequence quality score measured in the Phred quality scale was above 30 for all the samples. The reads were mapped to the human genome (GRCh38) using the STAR software, version 2.3.1z²⁰. On average, 96.4% of the sequenced reads mapped to the genome, resulting between 24.3 and 32.8 million mapped reads per sample, of which on average 89% were uniquely mapped reads. Transcript abundance estimates were calculated using HTSeq (version 0.6.1)²¹. Expression normalization and differential gene expression calculations were performed in edgeR (release 2.14)²² to identify statistically significant differentially expressed genes. A paired sample design was used in edgeR, which employs a negative binomial generalized linear model for statistical calculations. The edgeR package implements advanced empirical Bayes methods to estimate gene-specific biological variation under minimal levels of biological replication. The RNA composition in each sample was normalized in edgeR using the trimmed mean of M-values method. The significant *P*-values were adjusted for multiple hypotheses testing by the Benjamini and Hochberg method²³ as modified by Storey²⁴, providing a false discovery rate *q* value for each differentially expressed gene. Genes with an absolute fold difference ≥ 2 and *q* ≤ 0.05 were considered statistically significant.

RNA-Seq Analysis

RNA-seq data were organized in a Microsoft Excel table for subsequent analyses. These normalized read counts (counts per million) were used to calculate fold change between the pre-lesion and post-lesion samples, and the log base 2 of fold change was used for further analysis.

Correlation matrices and heat maps, as well as volcano plots, were generated in Excel. Functional overrepresentation analysis on the GO set of term annotations²⁵ was performed using DAVID pathway analysis²⁶. DAVID is an online software tool that groups genes based on their functional similarity. Given a list of significantly differentially expressed genes, DAVID uses a fuzzy clustering algorithm, that uses information in its knowledge base on genes and

their functional associations, to group genes that are together, statistically significant in their association to a set of common functional categories²⁶.

AmiGO GO annotations (<http://www.geneontology.org/>) for terms of interest were cross-referenced with significantly differentially expressed genes, yielding a list of differentially expressed genes related to each GO annotation's respective biological function. The GO annotations chosen to be visualized in heat maps were selected based on their relevance to peripheral nerve repair¹⁶. Statistical criteria of *q* ≤ 0.05 and $|FC| \geq 2$ were selected, yielding a total of 3,641 differentially expressed genes included in this analysis. Heat maps of the qualifying genes were generated using JMP Pro 13 (SAS). Hierarchical clustering was performed using Ward's method in JMP.

Results

Tissue Samples

The mass and freezing delay time (time from when the nerve was removed from participant to when it was snap-frozen in dry ice) were calculated for the pre-lesion and post-lesion tissue (Table 1). Freezing time delay was significantly longer (paired two tailed *t*-test: $t(5) = 4.863$, *P* = 0.004) for post-lesion nerve samples (59 \pm 25 min; mean \pm SD) than pre-lesion ones (18 \pm 5 min). This difference was a result of the longer surgical procedures needed for Stage II of the DBS surgery. The mitigation of Mass Effect during the RNA Access library preparation was accomplished in multiple ways through normalizations incorporated at multiple steps through the entire process of library preparation and sequencing.

Correlation Matrix and Volcano Plot

Analysis of the samples showed statistically significant changes in RNA levels among all six participants in response to the nerve transection lesion (Fig. 2A), with significant differences between the pre- and post-lesion samples and similarities within each of these groups as assessed by Pearson *r* correlation.

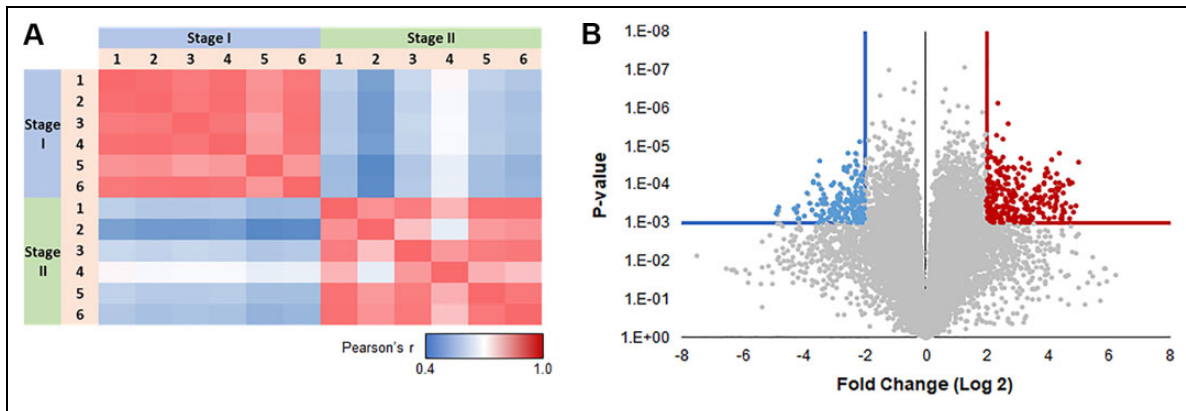


Fig. 2. (A) Correlation matrix or Pearson's r for the transcriptional profile of every subject vs every other subject. Scale bar: Correlation values range from 0.4 (blue—less similar) to 1 (red—more similar). This visualization shows strong agreement among different profiles within each stage, and a sharp distinction between stages. (B) Differences between Stage 1 and Stage 2. Log₂ scale fold changes (x -axis) are plotted as a function of P -value (inverted log₁₀ scale—volcano plot). Results that exceed conservative q -value ($q \leq 0.0003$) and fold change ($|\text{FC}| \geq 4$) cutoffs are highlighted (blue—downregulated in Stage 2, red—upregulated in Stage 2). FC: fold change.

The Volcano plot (Fig. 2B) estimates the most meaningful changes in the gene transcriptome, between pre- and post-lesion that exceeded a cutoff of $q \leq 0.0003$ and fold change $|\text{FC}| \geq 4$. Of those significantly differentially expressed genes, 693 gene transcripts (orange) were increased and 576 gene transcripts were decreased (blue). This analysis demonstrates that even with a very conservative criterion, there were hundreds of differentially expressed genes between the pre- and post-lesion tissue samples.

DAVID Pathway Analysis

DAVID pathway analysis revealed that the majority of the most significantly upregulated pathways (Table 2) were related to cell cycle, cell proliferation, and immune cell function. The majority of the most significantly downregulated pathways (Table 3) were related to synaptic structure and neuron function.

Growth Factor Activity

Figure 3 shows all significantly differentially expressed ($q < 0.05$, $|\text{FC}| > 2$) gene transcripts annotated with the Gene Ontology (GO) term “Growth Factor Activity” (GO:0008083). Out of 166 unique genes with this GO annotation, 43 (25.9%) were significantly differentially expressed between pre- and post-lesion. Twenty-six of those genes were more abundant, whereas 17 genes were less abundant in post-lesion tissue in comparison with pre-lesioning levels.

Myelination

Figure 4 shows all significantly differentially expressed ($q < 0.05$, $|\text{FC}| > 2$) gene transcripts annotated with the GO term “Myelination” (GO:0042552). Out of 110 unique genes with this GO annotation, 48 genes (43.6%) were significantly

differentially expressed. Seven genes were more abundant and 41 genes were less abundant in response to the injury.

Schwann Cell Transdifferentiation

Using the GO term “Epithelial–Mesenchymal Transition” (GO:0001837), 130 unique genes were yielded (Fig. 5). Of these, 29 genes (22.3%) were significantly differentially expressed (24 genes were more abundant and 5 genes were less abundant in post-lesion samples than pre-lesion samples). Likewise, the GO term “Schwann Cell Differentiation” (GO:0014037) identified 36 unique genes. Of these genes, 15 (41.7%) were significantly differentially expressed, with only 1 gene being more abundant while the other 14 genes less abundant in Stage II samples than Stage I samples.

Neuroprotection

“Negative Regulation of Apoptotic Processes” is defined by “Any process that stops, prevents, or reduces the frequency, rate or extent of cell death by apoptotic process.” And Negative Regulation of Neuron Death is defined as “any process that stops, prevents or reduces the frequency, rate or extent of neuron death.” Figure 6 shows all significantly differentially expressed gene transcripts annotated with the GO term “Negative Regulation of Apoptotic Processes” (GO:0043066) or “Negative Regulation of Neuron Death” (GO:1901215). This ontology yielded 916 unique genes, of which 128 (14.0%) were significantly differentially expressed (all 128 genes were more abundant in Stage II samples than in Stage I samples). Meanwhile, for Negative Regulation of Neuron Death, we found 67 genes out of 206 (32.5%) were significantly differentially expressed (45 genes more abundant and 22 genes less abundant in post-lesion samples than in pre-lesion samples). These gene changes indicated significant increases in transcripts of genes related to the reduction of neuron death.

Table 2. Top Significantly Increased Gene Ontology (GO) Pathways During Regeneration.

GO ID	GO term	Number of gene transcripts	P-value
GO:0000278	Mitotic cell cycle	83	2.42E-32
GO:0007067	Mitotic nuclear division	57	3.97E-31
GO:0000819	Sister chromatid segregation	41	1.20E-27
GO:0044770	Cell cycle phase transition	49	4.75E-19
GO:0071103	DNA conformation change	32	1.21E-16
GO:0002682	Regulation of immune system process	62	4.67E-14
GO:0000228	Nuclear chromosome	41	3.38E-13
GO:0006952	Defense response	58	1.11E-11
GO:1901987	Regulation of cell cycle phase transition	29	5.00E-11
GO:0051303	Establishment of chromosome localization	14	2.42E-10
GO:0006259	DNA metabolic process	46	4.49E-09
GO:0002366	Leukocyte activation involved in immune response	19	6.52E-09
GO:0042129	Regulation of T cell proliferation	16	1.64E-08
GO:0051321	Meiotic cell cycle	17	2.41E-07
GO:0006342	Chromatin silencing	13	5.18E-07
GO:0033043	Regulation of organelle organization	46	5.84E-07
GO:0032640	Tumor necrosis factor production	12	7.16E-07
GO:0000910	Cytokinesis	13	1.42E-06
GO:0046631	Alpha-beta T cell activation	12	2.69E-06
GO:0001932	Regulation of protein phosphorylation	45	3.85E-06
GO:0006302	Double-strand break repair	16	6.15E-06
GO:0007051	Spindle organization	12	1.01E-05
GO:0050663	Cytokine secretion	13	1.54E-05
GO:0032101	Regulation of response to external stimulus	28	2.78E-05
GO:0032675	Regulation of interleukin-6 production	10	2.86E-05
GO:0019899	Enzyme binding	54	3.65E-05
GO:0060089	Molecular transducer activity	35	3.80E-05
GO:0044774	Mitotic DNA integrity checkpoint	11	5.42E-05
GO:0006270	DNA replication initiation	7	5.53E-05
GO:0002704	Negative regulation of leukocyte-mediated immunity	7	6.60E-05
GO:0032760	Positive regulation of tumor necrosis factor production	8	7.62E-05
GO:0034501	Protein localization to kinetochore	5	8.20E-05
GO:0009897	External side of plasma membrane	14	8.27E-05

Table 3. Top Significantly Decreased Gene Ontology (GO) Pathways During Regeneration.

GO ID	GO term	Number of gene transcripts	P-value
GO:0042391	Regulation of membrane potential	17	2.69E-08
GO:0098590	Plasma membrane region	27	4.06E-08
GO:0050803	Regulation of synapse structure or activity	14	8.01E-08
GO:0050877	Neurological system process	22	7.00E-07
GO:0050808	Synapse organization	13	8.20E-07
GO:0048812	Neuron projection morphogenesis	18	4.23E-06
GO:0030426	Growth cone	10	1.42E-05
GO:0050807	Regulation of synapse organization	8	4.21E-05
GO:0034765	Regulation of ion transmembrane transport	13	5.56E-05
GO:0005578	Proteinaceous extracellular matrix	13	6.25E-05
GO:0035725	Sodium ion transmembrane transport	8	7.87E-05
GO:0098794	Postsynapse	13	9.39E-05

Discussion

These results provide evidence that the transection lesion paradigm used in these surgeries induces phenotypic changes in the peripheral nerve tissue consistent with the peripheral nerve repair response: immune cell infiltration

plus cell proliferation, Wallerian degeneration of axons, cessation of myelin synthesis, and upregulation of growth factors production^{16,27,28}. DAVID pathway analysis revealed significant changes in genes related to the cell cycle, cell proliferation, immune cell function, synaptic structure, and

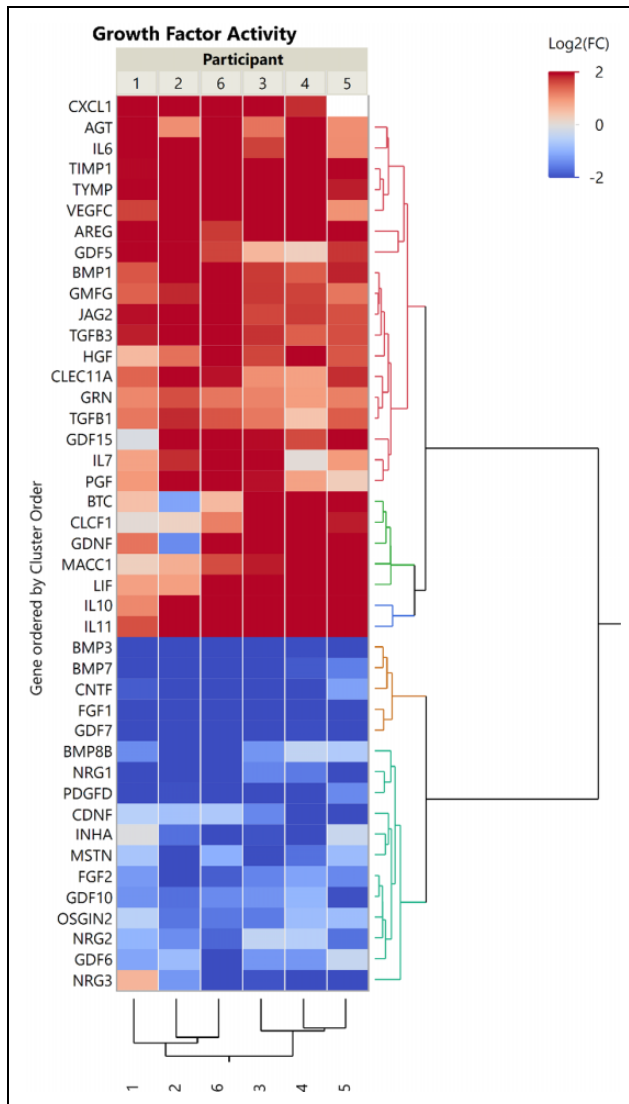


Fig. 3. Heat map showing all significantly differentially expressed ($q < 0.05$, $|FC| > 2$) gene transcripts annotated with the GO term “Growth factor Activity” (GO:0008083). Genes are organized by Ward hierarchical clustering. Dendrograms are scaled to hierarchical clustering distance; longer branches represent more distant clusters. FC: fold change; GO: gene ontology.

neuron function. In addition, significant decreases in myelination-related gene transcripts were observed. The majority of significantly differentially expressed genes related to growth factor activity were upregulated, and of particular note was the expression of the GDNF gene. GDNF is known to promote neuroprotection and/or neurorestoration in the CNS and has been studied as a therapeutic for PD, reaching Phase I and II clinical trials in humans^{29–31}. These results also demonstrated a loss of markers of mature Schwann cell phenotype (MYOC³², FA2H³³) while those of the epithelial–mesenchymal transition increased (SNAI2³⁴, WNT2³⁵). Taken together, these results indicate that the transection injury paradigm used in these human surgeries

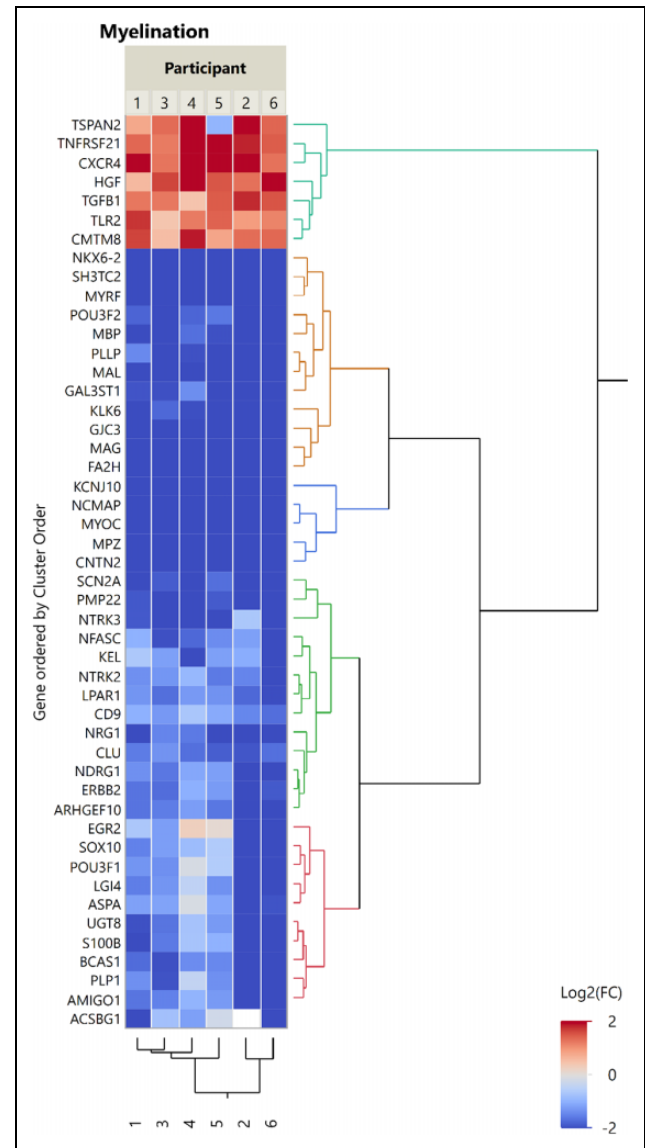


Fig. 4. Heat map showing all significantly differentially expressed ($q < 0.05$, $|FC| > 2$) gene transcripts annotated with the GO term “Myelination” (GO:0042552). Genes are organized by Ward hierarchical clustering. Dendrograms are scaled to hierarchical clustering distance; longer branches represent more distant clusters. FC: fold change; GO: gene ontology.

induced the transdifferentiation or reprogramming of peripheral nerve Schwann cells from a mature (myelinating) form into a repair (demyelinating) phenotype.

To better refine the results of our RNA-seq analysis to a more “biologically relevant” dataset, we decided to limit our observations to the genes whose transcript levels exceeded a fold change threshold of $|FC| > 2$. However, this convention may exclude genes that are biologically relevant at lower fold changes. For example, the transcription of NF2 gene, a marker of Schwann cell proliferation, was statistically significantly increased (P -value = 0.0192). However, the fold

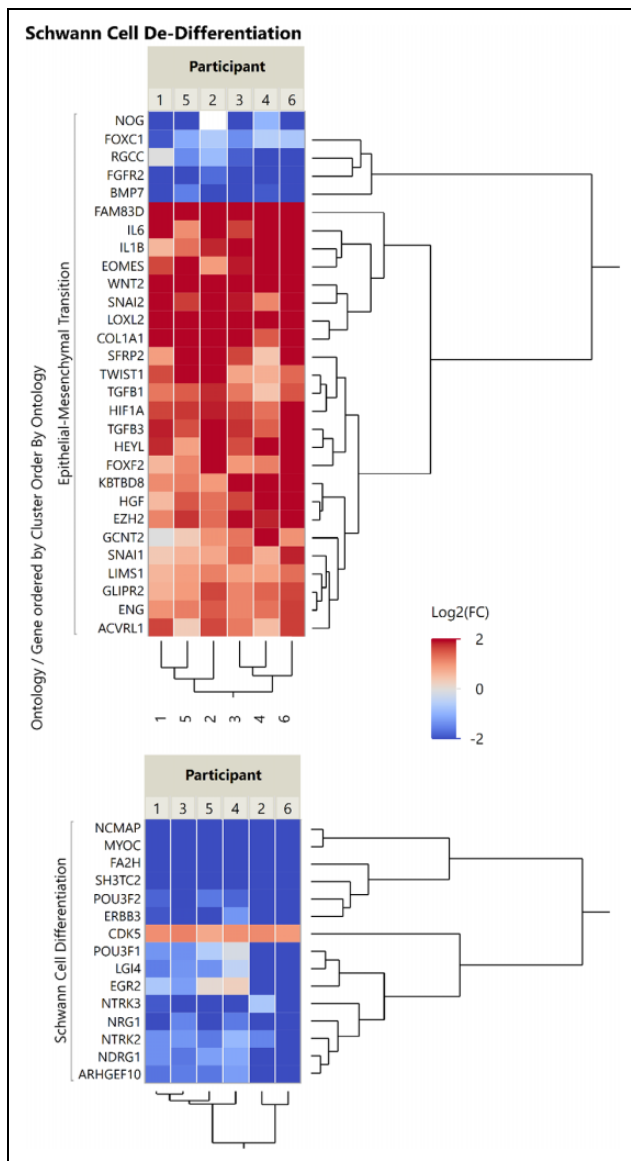


Fig. 5. Heat map showing all significantly differentially expressed ($q < 0.05$, $|FC| > 2$) gene transcripts annotated with the GO term “Epithelial–Mesenchymal Transition” (GO:0001837) or “Schwann Cell Differentiation” (GO:0014037). Genes are organized by Ward hierarchical clustering. Dendrograms are scaled to hierarchical clustering distance; longer branches represent more distant clusters. FC: fold change; GO: gene ontology.

change of transcript levels was less than 2, so it was not included in the visualized data. Likewise, Mesencephalic Astrocyte Derived Neurotrophic Factor (MANF) transcripts level was significantly higher postinjury (P -value = $3.03E-07$), yet its FC was 1.754 (data not shown). MANF plays a vital role in different reparative phases during the neuronal regeneration processes³⁶, and MANF therapeutics are expected to enter clinical trials. Furthermore, we focused in this article only on transcripts that were differentially expressed between pre- and post-lesion samples while

recognizing that some genes could be highly expressed in both stages, but not necessarily differentially. This is one limitation of this broad analysis approach, and in the specific case of NF2 levels in this tissue merits further study. The visualization of the negative regulation of apoptotic processes was also striking because over 100 genes were significantly differentially expressed and all were upregulated. This suggests that marked suppression of apoptosis was occurring in this tissue. Whether these antiapoptotic processes confer neuroprotection after tissue grafting merits further study.

The gene cluster of the growth factor terms showed multiple differentially expressed genes, with the majority being increased. One increased gene of note is GDNF, which is neuroprotective and neurorestorative of dopaminergic neurons and has been tried as a therapeutic intervention for PD^{29,31,37,38}. All post-lesion nerve samples, except one, demonstrated an upregulation of GDNF transcription. Only the nerve sample collected from participant number 2 demonstrated a lower number of GDNF transcripts after injury (Fig. 3). The significant longer freezing time delay for this sample (Table 1) might have negatively affected GDNF-mRNA stability and its relevant count during RNA-seq processing. Multiple interleukins were also upregulated which, in addition to being cytokines, play a role in neurogenesis (for review, see Borsini et al³⁹). For example, the levels of gene transcript for IL-6, which has been described as neuroprotective against focal brain injury, were increased in response to the nerve injury⁴⁰. The growth factor activity genes, which were decreased (e.g., CDNF) at 2 weeks post-injury are also of interest and may indicate the complexity of the neuronal repair process in regard to the changes of individual growth factors over time in response to nerve injury. That was evident in the work of Lin et al⁴¹ as PPAR, PI3K-Akt, and chemokine signaling pathways were dominant in early Wallerian degeneration. Whereas at the later stage, the main signaling pathways were ErbB, tumor necrosis factor, AMPK, MAPK, PPAR, and Wnt⁴¹.

To our knowledge only Weiss and colleagues⁴² have performed RNA-seq analysis on human peripheral nerve fascicles. They studied human peripheral nerve fascicles collected during surgeries, ex vivo degenerated nerves (for 8 d), cultured Schwann cells, and cultured fibroblasts. Their method of obtaining degenerated nerves differed from ours in that our model was degenerated in vivo and tissues were collected 2 weeks postinjury. Studies in animal models are more common. Arthur-Farraj et al²⁸ reported transcriptome and DNA methylome findings from mouse models. They found changes in epithelial–mesenchymal transition, which we also observed. Yi et al⁴³ studied a rat model of sciatic nerve crush injury and showed at acute, subacute, and post-acute time points the expression of inflammation and immune response; cellular movement, development, and morphology; and lipid metabolism, cytoskeleton reorganization, and nerve regeneration were all upregulated, respectively. Of note both Arthur-Farraj et al. and Yi et al.

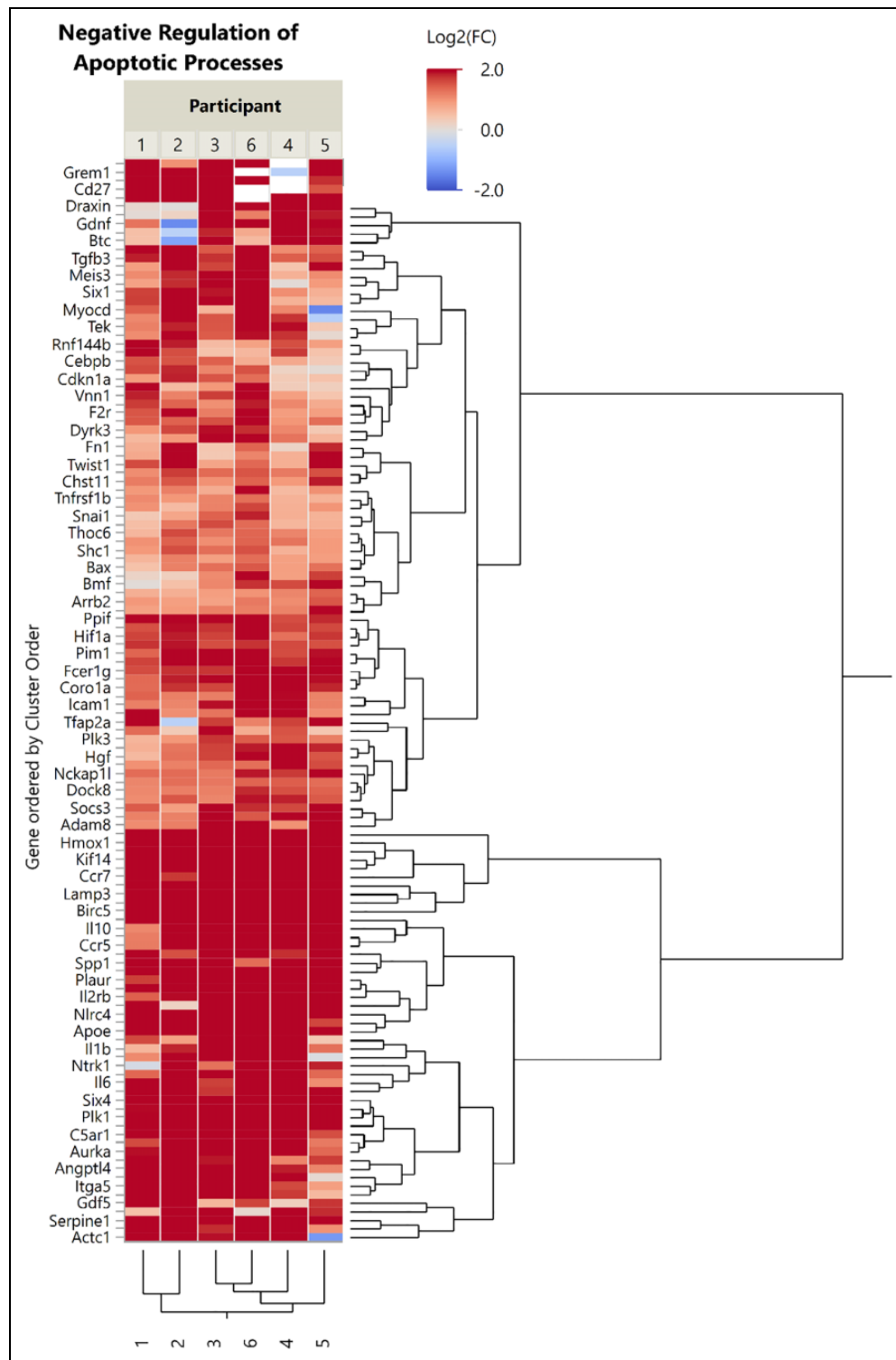


Fig. 6. Heat map showing all significantly differentially expressed ($q < 0.05$, $|FC| > 2$) gene transcripts annotated with the GO term “Negative Regulation of Apoptotic Processes” (GO:0043066) or “Negative Regulation of Neuron Death (GO:1901215).” Genes are organized by Ward hierarchical clustering. Dendrograms are scaled to hierarchical clustering distance; longer branches represent more distant clusters. FC: fold change; GO: gene ontology.

performed sequencing at multiple time points postinjury. This approach allowed them to show the change in differentially expressed pathways over time.

Myelination genes showed that significantly differentially expressed genes of this ontology were decreased 2 weeks after injury. This is consistent with myelin

degradation after peripheral nerve injury as previously described⁴⁴. In general, the Schwann cells showed overall decreased transcripts related to differentiation. This could be interpreted as transdifferentiation or reprogramming of Schwann cells²⁷. However, this comparison was not straightforward. We expected to see that the JUN gene, which codes for the c-Jun transcription factor that regulates Schwann cell transdifferentiation, would be increased²⁷. We found that the JUN gene was not significantly differentially expressed in these samples. We currently hypothesize that the time course of JUN transcription did not match with the two samples taken 2 weeks apart, as previous studies have identified increased JUN levels at 1 week post-lesion²⁸. In fact, this study is limited overall in that it only addresses the levels of gene transcripts in the fascicles 2 weeks after the injury. Ideally, future studies should strive to investigate both shorter (3 to 7 days) and longer (3 to 6 weeks) postinjury periods to better understand the transdifferentiation process and the time course of the repair code.

The participants who donated tissue for this study had all been diagnosed with idiopathic PD and it is possible that the disease processes of this neurodegenerative disorder had some effect on peripheral nerve gene expression and its injury response, though this is not described in the available scientific literature. In other participants of the clinical trial (not included here), who have had a history of neuropathy, we have used clinical nerve conduction velocity tests to assess the sural nerve before grafting. None of those participants showed remarkable decrements in nerve conduction velocity (data not shown). A future study comparing baseline levels of RNA in patients with PD versus age-matched healthy controls could help determine potential baseline differences.

Because the underlying clinical trial necessitates a full transection of the sural nerve and excision of approximately 3 to 5 cm, participants commonly reported a painful sensation immediately postoperatively followed by numbness or tingling on the lateral aspect of the ankle and/or foot even after 1 yr. However, participants have not reported the sensation as painful or bothersome. The use of sural nerve excision in neurosurgical and plastic surgery applications has a robust literature and is shown to be well tolerated^{45,46}.

With regard to the influence of variation of age and degree of PD within the study group, there was a remarkable consistency of transcriptome profiles within the pre- and post-lesion groups as assessed by the Pearson *r* correlation. The transcriptome profile of all participants in the pre-lesion group was similar, as was the transcriptome profile of all participants in the post-lesion group. The histology and transcriptome profiles of the peripheral nerve tissue in response to an injury were consistent with previous reports^{28,42,43}. Furthermore, the correlation matrix visualizes the consistent RNA levels between participants as a result of the pre-lesioning approach^{15,17}. These results support consistent transcriptome changes within the study group. Furthermore, these results support the feasibility and reproducibility of the

time delayed approach for producing transdifferentiation of the sural nerve tissue into a repair cell phenotype in subjects with PD.

The freezing time delay difference between pre- and post-lesion samples is one of the limitations with the design of our study. This was inherent to the trial design where the focus was to optimize the surgical grafting procedure and the availability of tissue to be grafted during the DBS surgery. In Stage I the tissue was processed to isolate the fascicles immediately after extraction. During Stage II, the fascicles were removed from the sural nerve tissue, placed on saline ice, the sural nerve incision was closed, the graft locations in the brain were targeted, and the fascicle tissue was then grafted into the patient. We recognize that this delay was reflected in the difference in freezing time between the stages and it added to the variability between the samples. As a result, some of the transcriptome measurements might have been affected especially in the post-lesion samples compared to the *in vivo* state. Additionally, this analysis of peripheral nerve repair is in the context of a full transection injury. Other injury modalities, e.g., crush injuries, have been shown to induce different repair processes than transection injury⁴⁷. One key difference is that while both crush and transection injury lead to Wallerian degeneration distal to the injury, in a crush injury the extracellular matrix scaffold remains intact, while this scaffold is interrupted in transection injury⁴⁸. This should be considered when applying these findings to other injury models.

The sural nerve fascicles analyzed by RNA-seq included all cells and tissue components within the peripheral nerve. It should be noted that the tissue analyzed does not include the epineurium of the sural nerve. This was intentional, as it reflects the graft tissue composition (fascicles only), which is intended to contain mostly Schwann cells, macrophages, and extracellular matrix. This yielded an aggregate of all RNA in the tissue from multiple cell types. A future study using single-cell RNA-seq would be able to investigate the responses of individual peripheral nerve cells and cell types. Thus, it is possible that while we have emphasized the importance of the Schwann cells in the RNA-seq data and the “repair cell” properties of the tissue that the results cannot at this time be solely attributed to changes in Schwann cells. Furthermore, while Weiss et al. validated RNA-seq information using proteomics, this study focused on transcriptome changes in the peripheral nerve in response to injury but did not assess protein changes. Future studies could shed additional light as to the *in vivo* response of peripheral nerve in response to injury as well as the relationship of the transcriptome to the proteome of this dynamic tissue.

Taken together, the results of this study present whole-tissue transcriptome-scale data about the Wallerian degeneration affecting the distal stump of human peripheral nerve and at 2 weeks postinjury. The findings of this study reveal significant changes in the transcriptome of an injured human peripheral nerve after 2 weeks of repair processes *in situ*.

Finally, this study provides data for future researchers to analyze and incorporate within their bioinformatics models of Wallerian degeneration. Such models may strengthen our understanding of the peripheral nerve repair process and its relevance to basic science as well as clinical and translational research that are looking to adapt peripheral nerve tissue/cells for use in promoting neuroprotection, neural repair, and regeneration for disorders of the CNS.

Acknowledgments

Special thanks to Clark Bloomer and the University of Kansas Medical Center Genomics Core.

Ethical Approval

The study was approved by the University of Kentucky Institutional Review Board (#44749).

Statement of Human and Animal Rights

Procedures were conducted in accordance with the University of Kentucky Institutional Review Board's (#44749) approved protocols.

Statement of Informed Consent

Written informed consent was obtained from participants for their anonymized information to be published.

Declaration of Conflicting Interests

The author(s) declared no potential conflicts of interest with respect to the research, authorship, and/or publication of this article.

Funding

The author(s) disclosed receipt of the following financial support for the research, authorship, and/or publication of this article: Ann Hanley Parkinson's Research Fund and the Clark Fund. The Genomics Core is supported by the following NIH grants—Kansas Intellectual and Developmental Disabilities Research Center (NIH U54 HD 090216), the Molecular Regulation of Cell Development and Differentiation—COBRE (P30 GM122731-03), the NIH S10 High-End Instrumentation Grant (NIH S10OD021743), and the Frontiers CTSA grant (UL1TR002366) at the University of Kansas Medical Center, Kansas City, KS, USA.

ORCID iD

Nader El Seblani  <https://orcid.org/0000-0002-4042-4890>

Supplemental Material

Supplemental material for this article is available online.

References

- Brushart TM. Nerve Repair. New York (NY): Oxford University Press; 2011.
- Sebille A, Bondoux JM. Motor function recovery after axotomy: enhancement by cyclophosphamide and spermine in rat. *Exp Neurol*. 1980;70(3):507–515.
- Oldfors A. Macrophages in peripheral nerves an ultrastructural and enzyme histochemical study on rats. *Acta Neuropathol*. 1980;49(1):43–49.
- Pellegrino RG, Politis MJ, Ritchie JM, Spencer PS. Events in degenerating cat peripheral nerve: induction of Schwann cell S phase and its relation to nerve fibre degeneration. *J Neurocytol*. 1986;15(1):17–28.
- Jessen KR, Arthur FP. Repair Schwann cell update: adaptive reprogramming, EMT, and stemness in regenerating nerves. *Glia*. 2019;67(3):421–437.
- Gaudet AD, Popovich PG, Ramer MS. Wallerian degeneration: gaining perspective on inflammatory events after peripheral nerve injury. *J Neuroinflammation*. 2011;8(1):110.
- Kidd GJ, Ohno N, Trapp BD. Biology of Schwann cells. *Handb Clin Neurol*. 2013;115:55–79.
- Jessen KR, Mirsky R. The repair Schwann cell and its function in regenerating nerves. *J Physiol*. 2016;594(13):3521–3531.
- Park JS, Hoke A. Treadmill exercise induced functional recovery after peripheral nerve repair is associated with increased levels of neurotrophic factors. *Plos One*. 2014;9(3):e90245.
- Hoke A, Redett R, Hameed H, Jari R, Zhou C, Li ZB, Griffin JW, Brushart TM. Schwann cells express motor and sensory phenotypes that regulate axon regeneration. *J Neurosci*. 2006;26(38):9646–9655.
- Henderson C, Phillips H, Pollock R, Davies A, Lemeulle C, Armanini M, Simmons L, Moffet B, Vandlen R, Simpson LC. GDNF: a potent survival factor for motoneurons present in peripheral nerve and muscle. *Science*. 1994;266(5187):1062–1064.
- Bunge RP. The role of the Schwann cell in trophic support and regeneration. *J Neurol*. 1994;242(1 Suppl 1):S19–S21.
- Fu SY, Gordon T. The cellular and molecular basis of peripheral nerve regeneration. *Mol Neurobiol*. 1997;14(1-2):67–116.
- Han Y, Gao S, Muegge K, Zhang W, Zhou B. Advanced Applications of RNA Sequencing and Challenges. *Bioinform Biol Insights*. 2015;9(Suppl 1):29–46.
- van Horne CG, Quintero JE, Slevin JT, Anderson-Mooney A, Gurwell JA, Welleford AS, Lamm JR, Wagner RP, Gerhardt GA. Peripheral nerve grafts implanted into the substantia nigra in patients with Parkinson's disease during deep brain stimulation surgery: 1-year follow-up study of safety, feasibility, and clinical outcome. *J Neurosurg*. 2018;129(6):1550–1561.
- Cattin AL, Lloyd AC. The multicellular complexity of peripheral nerve regeneration. *Curr Opin Neurobiol*. 2016;39:38–46.
- van Horne CG, Quintero JE, Gurwell JA, Wagner RP, Slevin JT, Gerhardt GA. Implantation of autologous peripheral nerve grafts into the substantia nigra of subjects with idiopathic Parkinson's disease treated with bilateral STN DBS: a report of safety and feasibility. *J Neurosurg*. 2017;126(4):1140–1147.
- van Horne CG, Vaughan SW, Massari C, Bennett M, Asfahani WS, Quintero JE, Gerhardt GA. Streamlining deep brain stimulation surgery by reversing the staging order. *J Neurosurg*. 2015;122(5):1042–1047.

19. Andrews S. 2010. FastQC: a quality control tool for high throughput sequence data. Available from <http://www.bioinformatics.babraham.ac.uk/projects/fastqc/> (accessed 4 May 2020).
20. Dobin A, Davis CA, Schlesinger F, Drenkow J, Zaleski C, Jha S, Batut P, Chaisson M, Gingeras TR. STAR: ultrafast universal RNA-seq aligner. *Bioinformatics*. 2013;29(1):15–21.
21. Anders S, Pyl PT, Huber W. HTSeq—a Python framework to work with high-throughput sequencing data. *Bioinformatics*. 2015;31(2):166–169.
22. Robinson MD, McCarthy DJ, Smyth GK. edgeR: a Bioconductor package for differential expression analysis of digital gene expression data. *Bioinformatics*. 2010;26(1):139–140.
23. Benjamini Y, Hochberg Y. Controlling the false discovery rate: a practical and powerful approach to multiple testing. *Journal of the Royal Statistical Society Series B*. 1995; 57(1):289–300.
24. Storey JD, Tibshirani R. Statistical significance for genome-wide studies. *Proc Natl Acad Sci U S A*. 2003;100(16): 9440–9445.
25. Harris MA, Clark J, Ireland A, Lomax J, Ashburner M, Foulger R, Eilbeck K, Lewis S, Marshall B, Mungall C, Richter J, et al. The Gene Ontology (GO) database and informatics resource. *Nucleic Acids Res*. 2004;32(Database issue):D258–D261.
26. Huang da W, Sherman BT, Lempicki RA. Systematic and integrative analysis of large gene lists using DAVID bioinformatics resources. *Nat Protoc*. 2009;4(1):44–57.
27. Arthur FPJ, Latouche M, Wilton DK, Quintes S, Chabrol E, Banerjee A, Woodhoo A, Jenkins B, Rahman M, Turmaine M, Wicher GK, et al. c-Jun reprograms Schwann cells of injured nerves to generate a repair cell essential for regeneration. *Neuron*. 2012;75(4):633–647.
28. Arthur FPJ, Morgan CC, Adamowicz M, Gomez SJA, Fazal SV, Beucher A, Razzaghi B, Mirsky R, Jessen KR, Aitman TJ. Changes in the coding and non-coding Transcriptome and DNA methylome that define the Schwann cell repair phenotype after Nerve injury. *Cell Rep*. 2017;20(11): 2719–2734.
29. Gill SS, Patel NK, Hotton GR, O’Sullivan K, McCarter R, Bunnage M, Brooks DJ, Svendsen CN, Heywood P. Direct brain infusion of glial cell line-derived neurotrophic factor in Parkinson disease. *Nat Med*. 2003;9(5):589–595.
30. Slevin JT, Gerhardt GA, Smith CD, Gash DM, Kryscio R, Young B. Improvement of bilateral motor functions in patients with Parkinson disease through the unilateral intraputamenal infusion of glial cell line—derived neurotrophic factor. *Journal of Neurosurgery*. 2005;102(2):216–222.
31. Whone A, Luz M, Boca M, Woolley M, Mooney L, Dharia S, Broadfoot J, Cronin D, Schroers C, Barua NU, Longpre L, et al. Randomized trial of intermittent intraputamenal glial cell line-derived neurotrophic factor in Parkinson’s disease. *Brain*. 2019;142(3):512–525.
32. Ohlmann A, Goldwisch A, Flugel-Koch C, Fuchs AV, Schwager K, Tamm ER. Secreted glycoprotein myocilin is a component of the myelin sheath in peripheral nerves. *Glia*. 2003;43(2):128–140.
33. Maldonado EN, Alderson NL, Monje PV, Wood PM, Hama H. FA2 H is responsible for the formation of 2-hydroxy galactolipids in peripheral nervous system myelin. *J Lipid Res*. 2008; 49(1):153–161.
34. Arima Y, Hayashi H, Kamata K, Goto TM, Sasaki M, Kuramochi A, Saya H. Decreased expression of neurofibromin contributes to epithelial-mesenchymal transition in neurofibromatosis type 1. *Exp Dermatol*. 2010;19(8): e136–e41.
35. Watson AL, Rahrman EP, Moriarity BS, Choi K, Conboy CB, Greeley AD, Halfond AL, Anderson LK, Wahl BR, Keng VW, Rizzardi AE, et al. Canonical Wnt/beta-catenin signaling drives human Schwann cell transformation, progression, and tumor maintenance. *Cancer Discov*. 2013; 3(6):674–689.
36. Sousa VP, Jasper H, Neves J. Trophic factors in inflammation and regeneration: the role of MANF and CDNF. *Frontiers in physiology*. 2018;9:1629.
37. Gash DM, Zhang Z, Ovidia A, Cass WA, Yi A, Simmerman L, Russell D, Martin D, Lapchak PA, Collins F, Hoffer BJ, et al. Functional recovery in parkinsonian monkeys treated with GDNF. *Nature*. 1996;380(6571):252–255.
38. Whone AL, Boca M, Luz M, Woolley M, Mooney L, Dharia S, Broadfoot J, Cronin D, Schroers C, Barua NU, Longpre L, et al. Extended treatment with glial cell line-derived neurotrophic factor in Parkinson’s disease. *J Parkinsons Dis*. 2019;9(2): 301–313.
39. Borsini A, Zunszain PA, Thuret S, Pariante CM. The role of inflammatory cytokines as key modulators of neurogenesis. *Trends Neurosci*. 2015;38(3):145–157.
40. Penkowa M, Giralt M, Lago N, Camats J, Carrasco J, Hernández J, Molinero A, Campbell IL, Hidalgo J. Astrocyte-targeted expression of IL-6 protects the CNS against a focal brain injury. *Exp Neurol*. 2003;181(2):130–148.
41. Lin YF, Xie Z, Zhou J, Yin G, Lin HD. Differential gene and protein expression between rat tibial nerve and common peroneal nerve during Wallerian degeneration. *Neural Regen Res*. 2019;14(12):2183–2191.
42. Weiss T, Taschner MS, Bileck A, Slany A, Kromp F, Rifatbegovic F, Frech C, Windhager R, Kitzinger H, Tzou CH, Ambros PF, et al. Proteomics and transcriptomics of peripheral nerve tissue and cells unravel new aspects of the human Schwann cell repair phenotype. *Glia*. 2016;64(12): 2133–2153.
43. Yi S, Zhang H, Gong L, Wu J, Zha G, Zhou S, Gu X, Yu B. Deep sequencing and bioinformatic analysis of Lesioned sciatic nerves after crush injury. *PLoS One*. 2015;10(12): e0143491.
44. Gomez SJA, Carty L, Iruarizaga LM, Palomo IM, Varela RM, Griffith M, Hantke J, Macias CN, Azkargorta M, Aurrekoetxea I, De JVG, et al. Schwann cell autophagy, myelinophagy, initiates myelin clearance from injured nerves. *J Cell Biol*. 2015; 210(1):153–168.

45. Strauch B, Goldberg N, Herman CK. Sural nerve harvest: anatomy and technique. *J Reconstr Microsurg.* 2005;21(2):133–136.
46. Butler DP, Johal KS, Wicks CE, Grobbelaar AO. Objective sensory and functional outcomes at the donor site following endoscopic-assisted sural nerve harvest. *J Plast Reconstr Aesthet Surg.* 2017;70(5):659–665.
47. Lago N, Navarro X. Correlation between target reinnervation and distribution of motor axons in the injured rat sciatic nerve. *J Neurotrauma.* 2006;23(2):227–240.
48. Caillaud M, Richard L, Vallat JM, Desmouliere A, Billet F. Peripheral nerve regeneration and intraneural revascularization. *Neural Regen Res.* 2019;14(1):24–33.